molecular human reproduction

ORIGINAL RESEARCH

The SEPT12 complex is required for the establishment of a functional sperm head–tail junction

Yi-Ru Shen[1,†], Han-Yu Wang[1,2,†], Yung-Chieh Tsai[3,4,5], Yung-Che Kuo[1,6], Shang-Rung Wu[7], Chia-Yih Wang[2,8,*], and Pao-Lin Kuo ⓘ [1,2,9,*]

[1]Department of Obstetrics and Gynecology, College of Medicine, National Cheng Kung University, Tainan, Taiwan [2]Institute of Basic Medical Sciences, College of Medicine, National Cheng Kung University, Tainan, Taiwan [3]Department of Obstetrics and Gynecology, Chi-Mei Medical Center, Tainan, Taiwan [4]Department of Medicine, Taipei Medical University, Taipei, Taiwan [5]Department of Sport Management, Chia Nan University of Pharmacy and Science, Tainan, Taiwan [6]TMU Research Center for Cell Therapy and Regeneration Medicine, Taipei Medical University, Taipei, Taiwan [7]Institute of Oral Medicine, College of Medicine, National Cheng Kung University, Tainan, Taiwan [8]Department of Cell Biology and Anatomy, College of Medicine, National Cheng Kung University, Tainan, Taiwan [9]Department of Obstetrics and Gynecology, National Cheng-Kung University Hospital, Tainan, Taiwan

*Correspondence address. Institute of Basic Medical Sciences, College of Medicine, National Cheng Kung University, Tainan, Taiwan. Tel: +886-6-2353535 ext. 5262; Fax: +886-6-2093007; E-mail: paolink@mail.ncku.edu.tw ⓘ http://orcid.org/0000-0002-0726-1030; Department of Cell Biology and Anatomy, College of Medicine, National Cheng Kung University, Tainan, Taiwan. Tel: +886-6-2353535 ext. 5338; Fax: +886-6-2093007; E-mail: b89609046@gmail.com ⓘ http://orcid.org/0000-0002-9196-0802

ABSTRACT: The connecting pieces of the sperm neck link the flagellum and the sperm head, and they are important for initiating flagellar beating. The connecting pieces are important building blocks for the sperm neck; however, the mechanism of connecting piece assembly is poorly understood. In the present study, we explored the role of septins in sperm motility and found that $Sept12^{D197N}$ knock-in (KI) mice produce acephalic and immotile spermatozoa. Electron microscopy analysis showed defective connecting pieces in sperm from KI mice, indicating that SEPT12 is required for the establishment of connecting pieces. We also found that SEPT12 formed a complex with SEPT1, SEPT2, SEPT10 and SEPT11 at the sperm neck and that the D197N mutation disrupted the complex, suggesting that the SEPT12 complex is involved in the assembly of connecting pieces. Additionally, we found that SEPT12 interacted and colocalized with γ-tubulin in elongating spermatids, implying that SEPT12 and pericentriolar materials jointly contribute to the formation of connecting pieces. Collectively, our findings suggest that SEPT12 is required for the formation of striated columns, and the capitulum and for maintaining the stability of the sperm head–tail junction.

Key word: septin / SEPT12 / acephalic sperm / connecting pieces / capitulum / striated columns / male fertility

Introduction

Human infertility occurs in ∼10–15% of couples, and approximately half of such cases are caused by male infertility (Jarow *et al.*, 2002). Among infertile men, spermatogenic failure is often observed. Thus, it is important to understand the molecular mechanisms by which spermatogenesis is regulated. Although many genetic and environmental factors have been implicated in spermatogenic failure, known factors causing male infertility can account for only 30–40% of patients in the andrology clinic (Krausz *et al.*, 2015; Krausz and Riera-Escamilla, 2018; Cannarella *et al.*, 2019). Therefore, it is

imperative to discover the regulatory pathways of spermatogenesis as well as relevant genes.

Septins (SEPTs), which belong to a GTPase family, play important roles in development and growth. The human septin family comprises four subgroups: SEPT2 subgroup (SEPT1, SEPT2, SEPT4 and SEPT5); SEPT3 subgroup (SEPT3, SEPT9 and SEPT12); SEPT6 subgroup (SEPT6, SEPT8, SEPT10, SEPT11 and SEPT14); and SEPT7 subgroup (SEPT7) (Sirajuddin *et al.*, 2009). By polymerizing into hexameric or octameric core complexes, SEPTs perform their functions by assembling oligomeric core complexes into filaments and bundles or even into highly ordered ring structures (Kinoshita, 2003; Sirajuddin *et al.*,

---

†These authors contributed equally to this work.

2007). Due to their filamentous structure, SEPTs are currently recognized as the fourth component of the cytoskeleton.

At step 15 of mouse spermiogenesis, the SEPT12 complex is already located at the sperm neck (Shen *et al.*, 2017; Yeh *et al.*, 2019). In mature sperm, SEPT4, 7 and 12 are located at the annulus, a submembrane ring structure demarcating the midpiece and the principal piece of the sperm tail. The $Sept4^{-/-}$ and $Sept12^{+/-}$ male mice showed annulus disorganization (bent tail) as well as other morphological defects (Ihara *et al.*, 2005; Kissel *et al.*, 2005; Lin *et al.*, 2009). In humans, the annulus/septin ring is disorganized in spermatozoa from a subset of infertile men with asthenozoospermia (Sugino *et al.*, 2008; Lhuillier *et al.*, 2009). We have identified heterozygous mutations of *SEPT12* (T89M and D197N) in infertile men (Kuo *et al.*, 2012). In parallel to humans, $Sept12^{D197N}$ knock-in (KI) mice presented with bent tails (Kuo *et al.*, 2015). In addition to bent tails, bent necks also occur in spermatozoa of humans and mice carrying the D197N mutation (Kuo *et al.*, 2012, 2015). The connecting piece consists of the capitulum (Cp) and striated columns (SCs) (Tokuhiro *et al.*, 2009; Ounjai *et al.*, 2012). We hypothesized that the SEPT12 complex is involved in the establishment of sperm connecting pieces, and in this study, we found that $Sept12^{D197N}$ KI mice displayed a higher proportion of acephalic spermatozoa (15%) than wild-type (WT) or heterozygous spermatozoa (~5%). Electron microscopy analysis showed defective head–tail junctions of the sperm in KI mice, indicating that SEPT12 is required for the integrity of sperm head–tail junctions. We also found that SEPT12 formed complexes with SEPT1, SEPT2, SEPT10, SEPT11 and SEPT12 at the sperm neck and that the D197N mutation disrupted complex formation, suggesting that the SEPT12 complex is implicated in the assembly of head–tail junctions. Additionally, SEPT12 interacted and colocalized with γ-tubulin in elongating spermatids, a finding supporting the important role of SEPT12 in the formation of Cp and SCs during biogenesis of the connecting pieces. Taken together, these findings indicate that the SEPT12 complex is required for the establishment of sperm head–tail junctions and robust sperm function.

Materials and methods

Generation of $Sept12^{D197N}$ KI mice

Animal experiments were approved by the Institutional Animal Care and Use Committee (IACUC) of National Cheng Kung University. The generation of $Sept12^{D197N}$ mice has been described in our previous publication (Kuo *et al.*, 2015). In brief, a genomic fragment carrying the entire mouse *Sept12* locus was constructed in a bMQ-374d12 BAC clone (Sanger Institute, Cambridge, UK). The genomic fragment of *Sept12* was used to replace the WT allele of *Sept12* in 129Sv mouse embryonic stem cells. The missense mutation D197N (GAC to AAC) was introduced by PCR. The cell lines were injected into C57BL/6J blastocysts to generate chimeric mice. Male chimeric mice were mated with C57BL/6 females to pass the KI allele to their offspring. Homozygous $Sept12^{D197N/D197N}$ mice (F2) were produced by mating $Sept12^{D197N/+}$ mice (F1) with each other. Heterozygous and homozygous KI mice were identified by the genotyping of WT and KI mice.

Semen analysis and fertility test

Details of the mouse semen analysis have been described previously (Lin *et al.*, 2009). Briefly, mouse spermatozoa collected from the cauda epididymis of 12-week-old or older WT or KI mice were suspended in human tubal fluid medium (Irvine Scientific, Santa Ana, CA, USA). Sperm were immobilized by diluting them in water and were counted with a hemocytometer. A total of 200 sperm were counted under a microscope in duplicate to obtain an average percentage motility. Computer-assisted semen analysis (CASA) using an HTM-IVOS motility analyzer (Hamilton Thorne Research, Beverly, MA, USA) was applied to analyze slow, medium and rapid motility, sperm path velocity and curvilinear velocity. The motility was quantified as described (Nolan *et al.*, 2004). For the fertility test, two WT females were caged with one homozygous KI male. Copulation was determined by assessment of vaginal plugs every morning. Mice were mated for at least 4 months for confirmation of fertility.

DNA constructs, cell culture and transfection

The generation of SEPT1, SEPT2, SEPT10, SEPT11 and SEPT12 cDNA has been described previously (Kuo *et al.*, 2015). *SEPT12* deletions (aa1-158, 158-257 and 258-358) were generated by PCR amplification of the cDNA. The sequences were confirmed using Sanger sequencing. For transient transfection, malignant human testis pluripotent embryonal carcinoma NT2/D1 cells were cultured in DMEM (high glucose, Thermo Fisher Scientific, Waltham, MA, USA) supplemented with 10% fetal bovine serum (Thermo Fisher Scientific, Waltham, MA, USA) and 1% antibiotics. The cells were transfected with Lipofectamine® 2000 (Thermo Fisher Scientific, Waltham, MA, USA) and plasmids according to methods described previously (Kuo *et al.*, 2015).

Clinical information

This study was approved by the Institutional Review Board of National Cheng Kung University Hospital, Taiwan. From January 2005 to July 2007, we found the infertile men carrying the $SEPT12^{D197N}$ mutation with abnormal semen parameters. The detail information has been described previously (Kuo *et al.*, 2015).

Immunofluorescence staining of spermatozoa and testis histology

Immunofluorescence staining of spermatozoa and histological examination of the testes were performed according to methods described previously (Shen *et al.*, 2017). In brief, NT2/D1 cells were plated on coverslips and fixed with 4% formaldehyde in PBS for 5–10 min at room temperature. The mouse and human spermatozoa were spread on slides and fixed with 4% paraformaldehyde in PBS. Cells and sperm were permeabilized with Triton X-100, blocked with Antibody Diluent (Dako North America, Santa Clara, CA, USA), and incubated with the following primary antibodies at a 1:100 dilution: anti-SEPT1, anti-SEPT4, anti-SEPT7, anti-SEPT11 (Santa Cruz Biotechnology, Dallas, TX, USA); anti-SEPT2, anti-SEPT6 (Proteintech, Rosemont, IL, USA); anti-SEPT10 and anti-SEPT12 (Abnova, Taipei, Taiwan); and γ-tubulin (Merck, Darmstadt, Germany). The cells and sperm were stained with lectin peanut agglutinin (PNA)-conjugated Alexa Fluor, MitoTracker

Red 580 (Thermo Fisher Scientific, Waltham, MA, USA) or DAPI (Southern Biotech, Birmingham, AL). For histological examinations, the mouse testes were fixed overnight in Bouin's solution, then the tissue was sectioned into 5-µm thin slices, which were affixed to glass slides. The slides were deparaffinized, rehydrated and subjected to hematoxylin/eosin staining.

Transmission electron microscopy

Transmission electron microscopy (TEM) analysis was performed according to methods described previously (Shen *et al.*, 2017). In short, mouse spermatozoa were collected from the cauda epididymis and were prefixed with 2.5% glutaraldehyde at 4°C overnight, which was followed by postfixation in a 1% OsO_4 solution at room temperature for 1 h. After postfixation, the samples were washed three times with ddH2O, dehydrated using ethanol and propylene oxide, embedded in Epon at room temperature, and polymerized at 54°C for 1 day. The 80-nm sections were collected on grids, stained with lead citrate and uranyl acetate and examined by TEM (JEOL, Tokyo, Japan).

Immunoprecipitation assay and western blot analysis

After transfection and protein extraction, cell lysates were collected with 1× RIPA buffer (10×, Merck Millipore, 20-188, 0.5 M Tris-HCl, pH 7.4, 1.5 M NaCl, 2.5% deoxycholic acid, 10% NP-40 and 10 mM EDTA) and incubated with Dynabead-antibody complex (Thermo Fisher Scientific, Waltham, MA, USA) at 4°C overnight on a rotator. The Dynabeads were washed three times with wash buffer (100 mM Tris, 150 mM NaCl, 2 mM EDTA, 0.5% Tween-20 and 0.01% NP-40). After coimmunoprecipitation, the Dynabeads were denatured at 95°C for western blotting, which was used to measure protein levels. The blots were incubated with the following antibodies: anti-GFP, anti-Myc (1:5000, GeneTex, GTX113617, GTX115046); anti-FLAG (1:5000, Sigma-Aldrich, F1804) or anti-HA (1:5000, BioLegend, 901514). Green fluorescent protein (GFP) antibody recognizes the GFP fusion proteins. FLAG antibody recognizes DYKDDDDK-tag fusion proteins. HA antibody recognizes hemagglutinin tag fusion proteins.

Statistical analysis

All values were determined as mean ± SD. Data were analyzed for significant differences using the Student's *t*-test by Prism 7, and if a value of $P < 0.05$ or $P < 0.001$ was considered significant.

Results

D197N mutation in mice leads to sperm immobility, defective sperm neck structure and male infertility

The gross morphology of the testes of WT and $Sept12^{D197N}$ KI mice was indistinguishable (Fig. 1A). Analysis of testicular histology revealed a similar germ cell population in the mice with each genotype, which is consistent with the lack of significant difference in sperm counts between the different mice (Fig. 1B and C). These findings indicate a normal reproductive organ and sperm production in $Sept12^{D197N}$ mice. However, CASA showed a slight decrease in the number of rapid sperm and an increase in static sperm in heterozygous males (Fig. 1D, Supplementary Fig. S1). Notably, homozygous males displayed severe defects in sperm motility, and the majority of spermatozoa were completely immotile. Examination of the sperm head–tail conjunction revealed that homozygous KI males produced more acephalic spermatozoa than WT males (Fig. 1E). Collectively, $Sept12^{D197N/D197N}$ homozygous mice displayed defects in sperm motility and sperm head–tail junctions.

The head–tail junction of sperm of $Sept12^{D197N}$ KI mice was then examined by TEM (Fig. 1F). In WT spermatozoa, the head–tail junction comprised the Cp and the SC. In the mutant spermatozoa, a lack of SC and Cp or incomplete SC and partially formed Cp was observed. These results suggest that $Sept12^{D197N/D197N}$ sperm displayed defective head–tail junctions, leading to unstable head–tail attachment and the disruption of flagellum beat initiation.

Examination of the physiological impact of these changes showed that the KI mice were viable and visually similar to their WT siblings. $Sept12^{D197N}$ heterozygous KI males and homozygous KI females showed normal fertility (Table 1 and data not shown). In contrast, the $Sept12$ homozygous KI males were completely infertile, as shown by the mating of homozygous KI males with WT females for 6 months resulting in no litters of pups (Table I). In conclusion, $Sept12^{D197N}$ KI mice are sterile due to defective head–tail junctions.

SEPT12 localizes to the sperm neck during spermiogenesis

The beginning of the head–tail junction is first observed at the sperm neck in step 10 mouse spermatids, and it persists until it is fully developed in step 16 spermatids. To explore the role of SEPT12 in the developmental process of head–tail junctions, we investigated the SEPT12 expression pattern during spermiogenesis. Immunofluorescence showed that SEPT12 accumulated around the sperm neck in step 9 spermatids and further condensed in step 10–11 spermatids (Fig. 2). The timing and location of the SEPT12 signal correlated with the beginning of head–tail junction formation. In step 12–16 spermatids, a further stage of head–tail junction development, SEPT12 continually stayed at the sperm neck (Fig. 2). This is the location of the whole 'pre-annulus' structure at this stage, which migrates from the neck to the final annulus position. Thus, the SEPT12 expression pattern correlates with the timing of head–tail junction biogenesis.

Considering that the SEPT12 expression pattern is consistent with the developmental process of head–tail junctions, we next explored whether SEPT12 is involved in the formation of the building blocks of head–tail junctions. Cp and SC developed in close association with the proximal and distal centrioles. Thus, proteins that compose the Cp and SC should be associated with centrosomal proteins. Using immunoprecipitation analysis, we found that SEPT12 interacted with γ-tubulin, a 'pericentriolar material' (PCM) of the centrosome in NT2/D1 cells, which are a human testicular carcinoma cell line (Fig. 3A). To further analyze the interaction between SEPT12 and centrioles *in vivo*, the testes of SEPT12-transgenic mice were used for coimmunoprecipitation analysis. SEPT12-transgenic mice were generated by overexpressing a plasmid containing the full-length SEPT12 tagged with GFP. The expression of GFP-SEPT12 was driven by the endogenous SEPT12
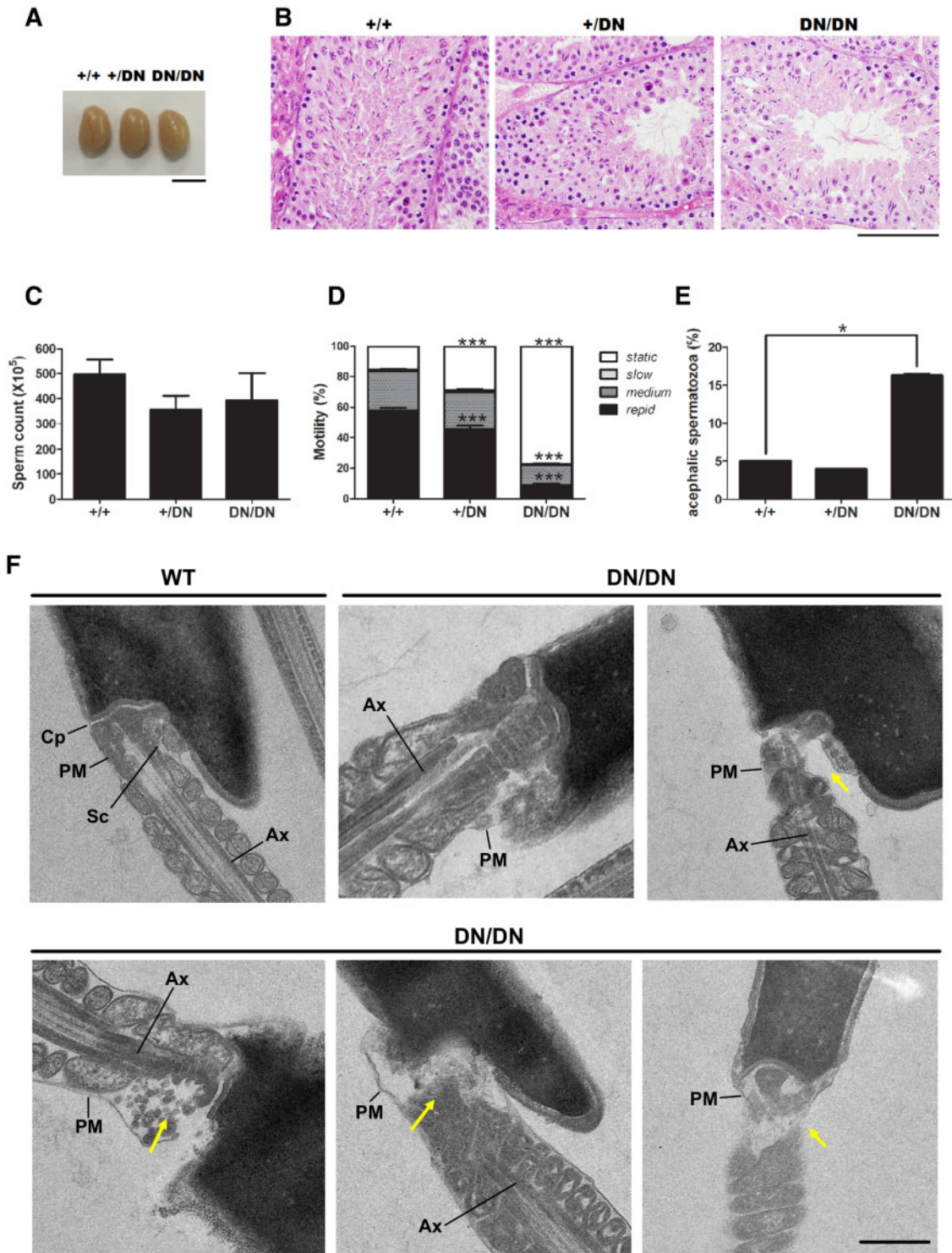
Figure 1 *Sept12$^{D197N/D197N}$* **(DN/DN) mice display defective sperm motility and acephalic spermatozoa.** (**A**) Gross morphology of the testes from wild-type (WT) and knock-in (KI) mice. Scale bar, 0.5 cm. (**B**) Hematoxylin and eosin staining of testicular sections of stage XII tubule sections from WT and KI mice. Scale bar, 100 μm. (**C**) Quantitative representation of WT and KI mutant sperm counts. Sperm were isolated from the cauda epididymis (the data represent mean ± SD from each genotype, N = 5). (**D**) Computer-assisted semen analysis of sperm motility (slow, medium and rapid motility) from the cauda epididymis of WT and KI mice (the data represent mean ± SD from each genotype, N = 5). ***P < 0.001 (Student's t-test). (**E**) Quantitative representation of acephalic sperm in WT and KI mutant caudal sperm (the data represent mean ± SD from each genotype, N = 5). *P < 0.05 (Student's t-test). (**F**) Transmission electron microscopy (TEM) analysis of sperm from the WT and KI mice. In the WT mice, the sperm neck is intact. In KI mice, the sperm neck is fractured, and the plasma membrane (PM) is disrupted. The striated columns (Sc) or capitulum (Cp) are either partially or completely absent in the mutant spermatozoa. Yellow arrows indicate the fractured neck. Ax, axoneme. Scale bar, 1 μm.

Table I Male fertility of SEPT12^{D197N} heterozygous and homozygous mice.

	No. of males	No. of mating females	Mating duration (months)	No. of litters delivered	No. of pups born	No. of pups per litter
SEPT12$^{+/D197N}$	5	10	6	51	288	5.65
SEPT12$^{D197N/D197N}$	5	10	6	0	0	0

Sept, septin.
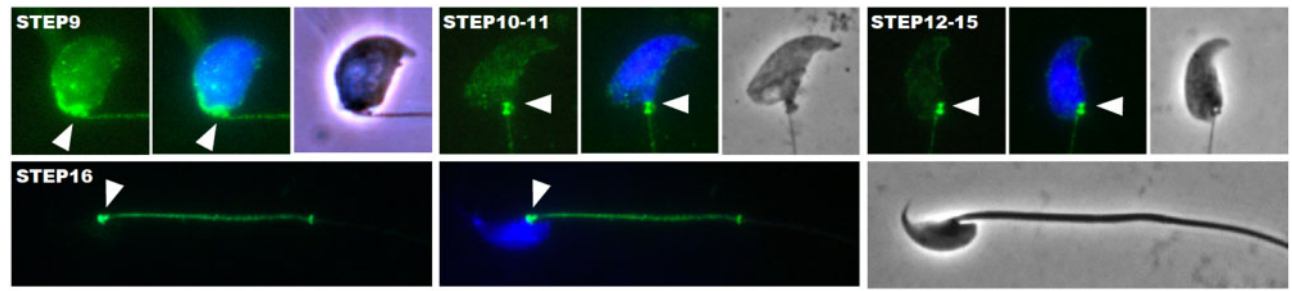
Figure 2 Immunofluorescence analysis of septin 12 in mouse spermatids at different developmental stages of spermiogenesis. The panels from left to right show the signals of SEPT12 (green), merged images of SEPT12 and DAPI (blue), and bright-field images (magnification: 1000×). White arrows indicate the sperm neck.

promoter. The data showed that γ-tubulin was coimmunoprecipitated with an anti-GFP antibody in testicular lysates of SEPT12-transgenic mice, indicating an association between SEPT12 and γ-tubulin *in vivo* (Fig. 3B). In addition, SEPT12 colocalized with γ-tubulin at the sperm neck in elongating spermatids (Fig. 3C). These data suggest that SEPT12 is associated with centrioles during head–tail junction formation. We further examined the interacting domains by using constructs containing truncated versions of SEPT12 in immunoprecipitation assays (Supplementary Fig. S2). The results showed that SEPT12 predominately interacted with γ-tubulin through its N-terminal region (aa 1-158) (Fig. 3D). Thus, SEPT12 interacted and colocalized with centrosomal protein *in vitro* and *in vivo*, and its association with γ-tubulin was via the N-terminal region. However, the D197N mutation did not influence the interaction with γ-tubulin (Supplementary Fig. S3), which is an expected finding given that the mutation is located within the GTP-binding pocket (Kuo *et al.*, 2012). Taken together, these findings suggest that SEPT12 is important for formation of the building blocks of Cp and SCs during biogenesis of the sperm head–tail junction.

SEPT12 forms a complex with SEPT1, SEPT2, SEPT10 and SEPT11 at the sperm head–tail junction

The physiological functions of septin highly depend on its ability to polymerize into complexes and filaments. We further investigated whether SEPT12 formed complexes at the sperm neck. In immunofluorescence analysis of human sperm, SEPT12 was localized at the caput pole of the midpiece, which is the location of the head–tail junction

(Fig. 4A). In addition, SEPT12 colocalized with SEPT1, SEPT2, SEPT10 and SEPT11 at the sperm head–tail junction (Fig. 4B). Given that SEPT12 interacts with SEPT1, SEPT2, SEPT10 and SEPT11, as shown by immunoprecipitation (Fig. 5A and B), SEPT12 may maintain head–tail junctions in a complex fashion.

D197N mutation disrupts SEPT12 filament formation

Next, we investigated the underlying head–tail junction defects in sperm carrying the D197N mutant, which lacks GTP-binding affinity. Considering that GTP-binding affinity is required for filament formation, we tested whether the D197N mutation disrupted the association of SEPT12 with SEPT1 and SEPT2, SEPT10 and SEPT11. Immunoprecipitation data revealed that the interactions of SEPT12^{D197N} with other SEPTs were dramatically or modestly decreased, indicating that the D197N mutation disrupted SEPT12 complex formation (Fig. 5C). Then we evaluated the integrity of the complex in the mutant sperm. In spermatozoa from a patient carrying the heterozygous D197N mutation, the SEPT12 and SEPT10 signals were retained in the neck but lost in the annulus. SEPT1 and SEPT11 signals were lost from both sites (Fig. 6A). In spermatozoa from the KI mouse, the SEPT12 signal was retained in the neck but was lost in the annulus. The SEPT1 signal was lost from both sites in the sperm of mice (Fig. 6B). Taken together, these results suggest that the D197N mutation disrupts the integrity of the SEPT complex and results in defective head–tail junctions of sperm.
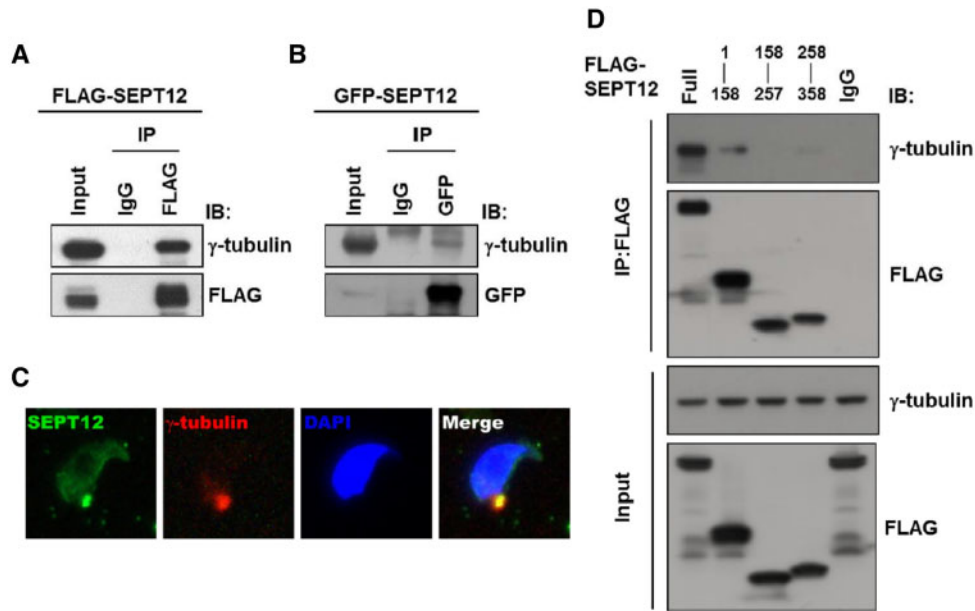
Figure 3 **SEPT12 interacts with γ-tubulin and colocalizes with γ-tubulin at the mouse sperm neck.** (**A**, **B**) Coimmunoprecipitation (IP) of green fluorescent protein (GFP)-SEPT12 with gamma-tubulin from NT2/D1 cells (A) and from SEPT12 transgenic mouse testes. Uncropped images are shown in Supplementary Fig. S4. (B) NT2/D1 cells were transfected with GFP-SEPT12 and the lysates were immunoprecipitated using an anti-GFP antibody. Immunoblotting was performed using anti-GFP and anti-gamma-tubulin antibodies. Uncropped images are shown in Supplementary Fig. S4. (**C**) Immunofluorescence analysis of SEPT12 and gamma-tubulin in spermatids (magnification: 1000×). The panels show the signals of SEPT12 (green), gamma-tubulin (red), DAPI (blue) and merged images from left to right. (**D**) SEPT12 interacts with gamma-tubulin mainly through aa 1-158. NT2/D1 cells were transfected with the FLAG (amino acid sequence motif: DYKDDDDK)-tagged full-length SEPT12 (Full) and various truncated versions of SEPT12. Coimmunoprecipitation of FLAG-SEPT12 with gamma-tubulin and western blotting was performed using anti-FLAG and anti-gamma-tubulin antibodies. Western blots of NT2/D1 whole cells extracts (input). Uncropped images are shown in Supplementary Fig. S5.

Discussion

Spermiogenesis is a maturation process that involves the development of sperm-specific organelles, and it results in terminally differentiated mature spermatozoa. During spermiogenesis, the Golgi complex develops into the acrosome, and mitochondria give rise to the mitochondrial sheath, which wraps around the axoneme to form the midpiece. Because spermatids do not enter mitosis, the centrosome undergoes a functional shift and begins serving as a platform for the assembly of the flagellar axoneme (Chemes and Rawe, 2010; Schlatt and Ehmcke, 2014). The centrosome of spermatids consists of a proximal centriole closely associated with the implantation fossa of the nucleus and a distal centriole engaged in the development of the axoneme (Schatten, 2012). In mammalian sperm, the flagellum is attached to the base of the head by the connecting pieces, which are composed of the SCs, basal plate and Cp (Soley, 2016).

Acephalic spermatozoa syndrome (MIM 617187) is characterized by ejaculate containing sperm with either decapitated flagella or tailless sperm heads and very few normal spermatozoa. This condition results from defects in the formation of the connecting piece of spermatozoa during late spermiogenesis (Chemes, 2018). The underlying defects of acephalic spermatozoa syndrome include failure of the proximal centrioles to attach to the caudal portion of the sperm nuclei and nuclear defects: the former results in misalignments of head and midpieces, while the latter interferes with formation of the implantation fossa, which is the lodging site for the sperm proximal centriole (Chemes et al., 1999; Rawe et al., 2002; Chemes and Alvarez Sedo, 2012). With abnormal development of the head–neck attachment, the sperm head and tail are usually separated during transit through the seminiferous tubules. Mouse models have revealed several genes involved in the production of acephalic spermatozoa, including coiled-coil domain containing 42 (Ccdc42) (Pasek et al., 2016), Centrobin (Liska et al., 2009), outer dense fiber protein 1 (Odf1) (Yang et al., 2012), ornithine decarboxylase antizyme 3 (Oaz3) (Tokuhiro et al., 2009), spermatogenesis-associated 6 (Spata6) (Yuan et al., 2015) and spermatogenesis and centriole associated 1 like (SPATC1L) (Kim et al., 2018). In humans, mutations of the Sad1 and UNC84 domain containing 5 (SUN5), polyamine modulated factor 1 binding protein 1 (PMFBP1), testis specific 10 (TSGA10), HOOK1 and bromodomain testis associated (BRDT) genes have been identified in infertile men with decapitated spermatozoa or acephalic spermatozoa syndrome (Zhu et al., 2016; Elkhatib et al., 2017; Li et al., 2017; Chen et al., 2018; Sha et al., 2018; Zhu et al., 2018). In this study, we found that homozygous D197N mutations of Sept12 resulted in completely immotile spermatozoa, ∼15% of which were decapitated spermatozoa. Notably, there was a lack of SC and Cp, or incomplete SC and partially formed Cp,
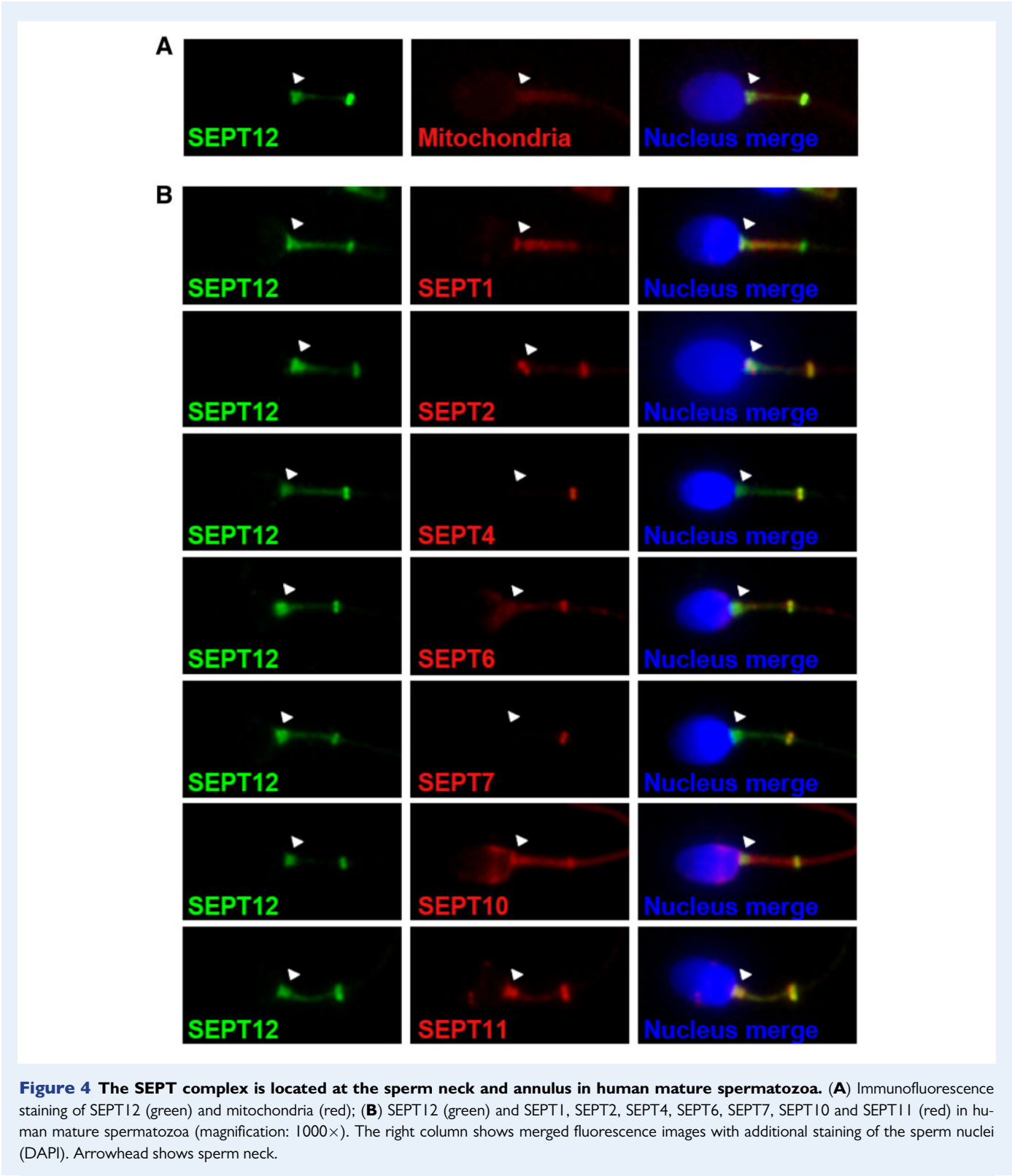
Figure 4 The SEPT complex is located at the sperm neck and annulus in human mature spermatozoa. (**A**) Immunofluorescence staining of SEPT12 (green) and mitochondria (red); (**B**) SEPT12 (green) and SEPT1, SEPT2, SEPT4, SEPT6, SEPT7, SEPT10 and SEPT11 (red) in human mature spermatozoa (magnification: 1000×). The right column shows merged fluorescence images with additional staining of the sperm nuclei (DAPI). Arrowhead shows sperm neck.

in the mutant spermatozoa. In humans, bent neck also occurs in men with heterozygous mutations in *SEPT12* (Kuo *et al.*, 2012). The sperm pathologies ranged from lack of SC and Cp to dysgenesis of these features in the mutant mouse. The low expressivity can be ascribed to

the redundancy of the septin family members. For example, *Sept6* KO mice were grossly normal and did not exhibit quantitative changes in any of the septins. Even the depletion of a close homolog of *Sept6*, *Sept11*, did not affect SEPT6-null cells *in vitro* (Ono *et al.*, 2005).
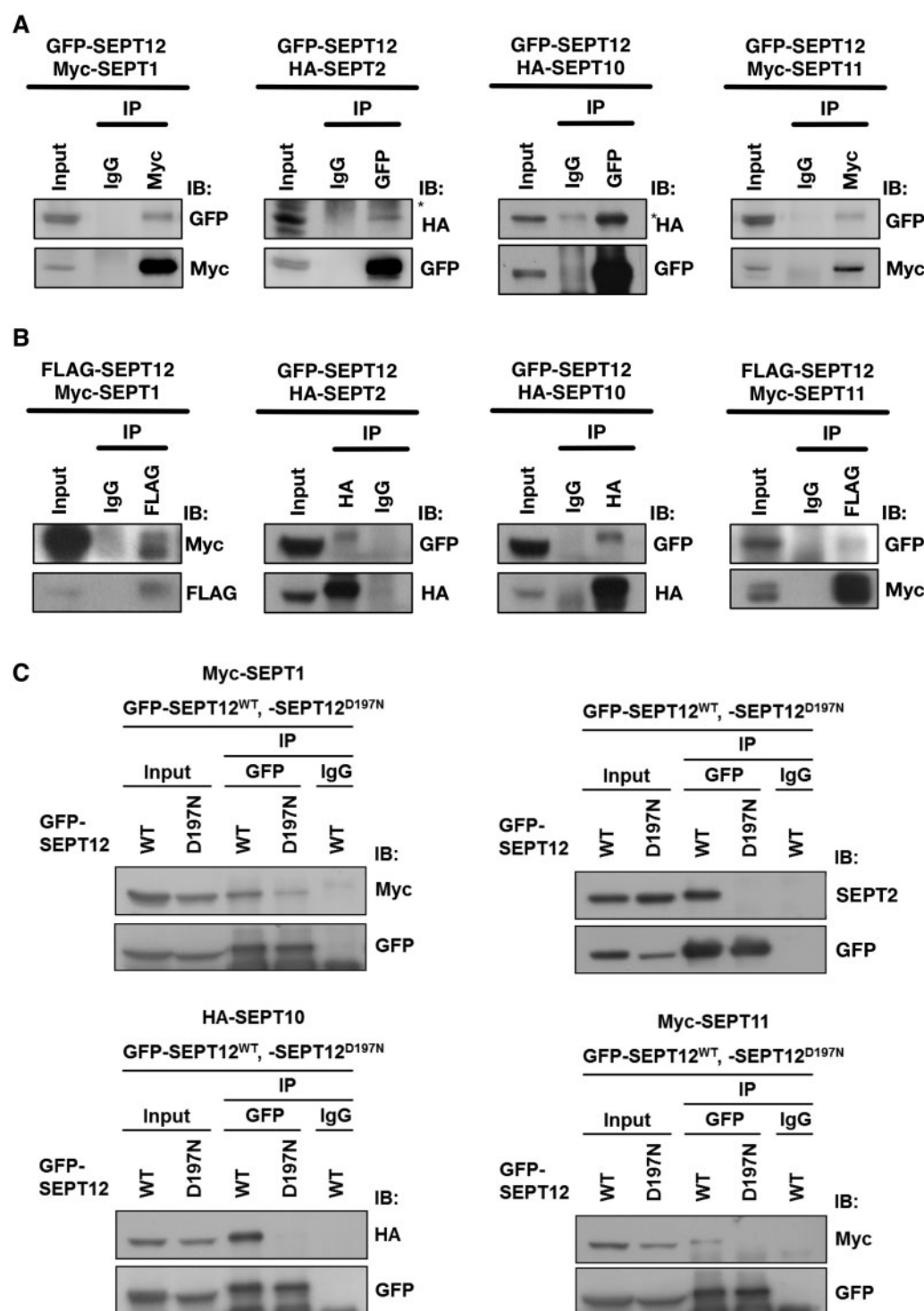
Figure 5 The D197N mutation dissociates SEPT12 from SEPT1, SEPT2, SEPT10 and SEPT11. (A) Coimmunoprecipitation of GFP-SEPT12 with Myc-SEPT1, Myc-SEPT11, HA-SEPT2 or HA-SEPT10. Uncropped images are shown in Supplementary Fig. S6. **(B)** The septin–septin interaction was confirmed by reciprocal immunoprecipitation. Uncropped images are shown in Supplementary Fig. S7. **(C)** Coimmunoprecipitation of GFP-SEPT12WT and GFP-SEPT12D197N with Myc-SEPT1, endogenous SEPT2, HA-SEPT10 or Myc-SEPT11. Western blotting was carried out with the indicated antibodies, as shown on the right. Western blots of NT2/D1 whole cells extracts (input). Uncropped images are shown in Supplementary Fig. S8.
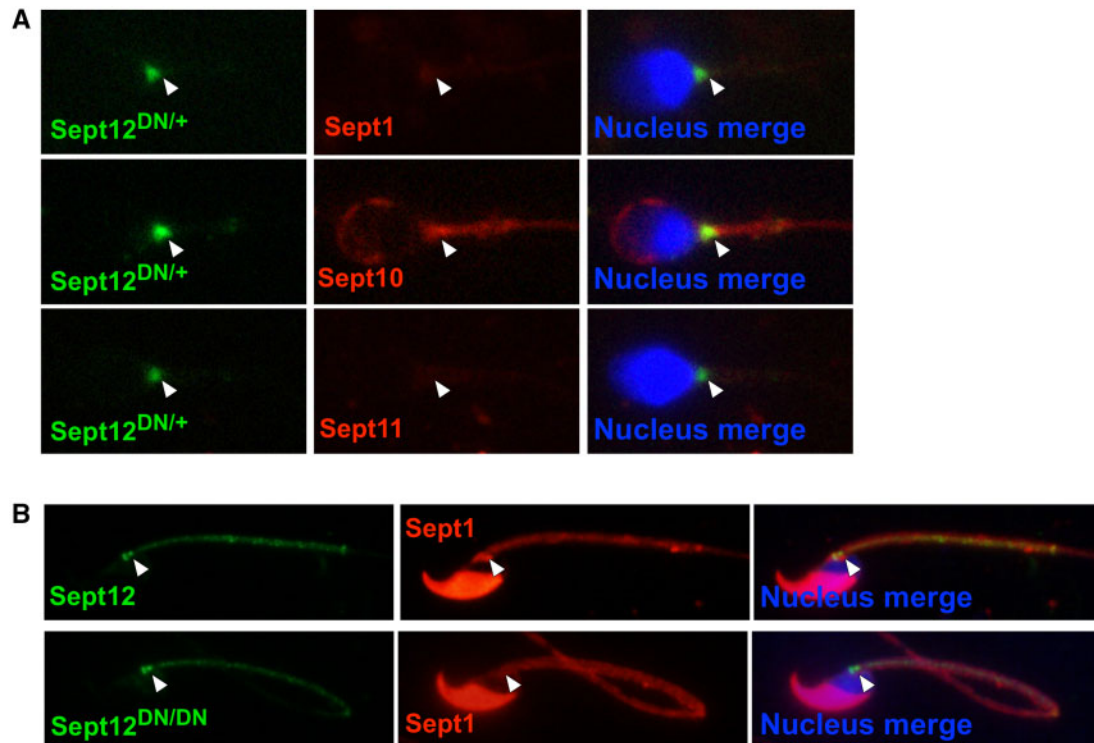
Figure 6 SEPT complex in mutant human and mouse sperm. (**A**) In human sperm, the SEPT12 and SEPT10 signals were retained in the neck but lost in the annulus. The SEPT1 and SEPT11 signals were lost from both sites (magnification: 1000×). (**B**) In mice, the SEPT12 signal was retained in the sperm neck but lost in the annulus. The SEPT1 signal was lost from both sites. The data for other SEPTs are not shown because those antibodies were not appropriate for immunofluorescence staining (magnification: 1000×). Nuclear staining (DAPI, blue). White arrows indicate the sperm neck.

Likewise, *Sept3* and *Sept5* KO mice did not exhibit overt phenotypes, implying a high degree of redundancy in the septin system (Tsang *et al.*, 2008).

The assembly of the connecting piece is organized by the proximal centrioles, whereas both flagellar axoneme and outer dense fibers (ODFs) originate from the distal centrioles (Schlatt and Ehmcke, 2014). SC represents a major structure of the connecting piece and has been suggested to arise from the so-called PCM (Schatten and Sun, 2009). In this study, the mutant spermatozoa exhibited a complete lack (agenesis) or partial lack (dysgenesis) of SC and Cp. By immunoprecipitation analysis, we found an association between SEPT12 and γ-tubulin *in vitro* and *in vivo*. This finding suggests that SEPT12/γ-tubulin jointly contributes to the formation of SC and the Cp. γ-tubulin is an essential component of the PCM. Fawcett *et al.* suggested that both centrioles appear to be involved in recruitment of the PCM during spermatid differentiation, while the PCM is converted into the SC and Cp of the connecting piece (Baccetti, 1970). However, in human sperm, only the proximal centriole is disassembled (Avidor-Reiss et al., 2019). Our observation that in the patient carrying the heterozygous D197N mutation, the SEPT12 and SEPT10 signals were retained in the neck (Fig. 6) might indicate that the SEPT12 complex is a component of distal centrioles. The link between SEPT12 and centrioles remains to be explored. Further work should also explore whether the

SEPT12 filament is involved in the recruitment of PCM or becomes a structural constituent of SC and Cp.

In this study, we showed that SEPT12 was colocalized with SEPT1, SEPT2, SEPT10 and SEPT11 at the sperm head–tail junction. Given that SEPT12 also interacted with SEPT1, SEPT2, SEPT10 and SEPT11, we reason that SEPT12 functions in the complex form in the sperm neck. Previously, we found that SEPT12 forms an octameric core complex with other SEPTs in the order of SEPT12–SEPT7–SEPT6–SEPT2/4–SEPT2/4–SEPT6–SEPT7–SEPT12 in the sperm annulus (Kuo et al., 2015). Phenotypic discrepancies exist between mice and humans. In this study, and in our previous work, mice with homozygous *Septin12* mutations displayed phenotypes comparable to infertile men who carried the heterozygous mutation. The discrepancy is probably due to species-specific numbers of spermatogenic stages, sperm morphology and spermatogenic efficiency (Borg et al., 2010). Notwithstanding this discrepancy, SEPT12 appears to form a distinct filament at the sperm neck in both species. We hypothesize that the mutant SEPT12 was anchored to γ-tubulin and retained at the sperm neck but not in the annulus given that the D197N mutation did not influence the interaction with γ-tubulin. However, it awaits further investigation of how the complex is assembled in the sperm neck.

Taken together, our findings suggest that SEPT12 is required for the formation of SC and the Cp and for maintaining the stability of the

sperm head–tail junction. We also identified a novel SEPT12 complex in the sperm neck of mice and human. Single gene mutations have been reported in various types of spermatogenic failures, including non-obstructive azoospermia, maturation arrest, asthenozoospermia and teratozoospermia (Cannarella et al., 2019). In a recent survey, a total of 521 disease–gene relationships were reported in spermatogenic failure, but some relationships remain questionable (Oud et al., 2019). We show that sperm neck pathology can be caused by SEPT12 mutations and extend the phenotypic spectrum of SEPT12 mutations.

Supplementary data

Supplementary data are available at Molecular Human Reproduction online.

Acknowledgments

Authors' roles

P.-L.K. and C.-Y.W. conceived and designed the experiments. Y.-R.S., Y.-C.K. and H.-Y.W. carried out the experiments and analyzed the data. All authors contributed to writing the manuscript. P.-L.K. and C.-Y.W. revised the final version of the draft.

Funding

Conflict of interest

There are no competing interests related to this study.

References

Avidor-Reiss T, Mazur M, Fishman EL, Sindhwani P. The role of sperm centrioles in human reproduction—the known and the unknown. Front Cell Dev Biol 2019;7:188–188.

Baccetti B. Comparative Spermatology: Proceedings of the International Symposium, Held in Rome and Siena, 1–5 July 1969. Rome: Accademia Nazionale dei Lincei, 1970, 13–22.

Borg CL, Wolski KM, Gibbs GM, O'Bryan MK. Phenotyping male infertility in the mouse: how to get the most out of a 'non-performer'. Hum Reprod Update 2010;16:205–224.

Cannarella R, Condorelli RA, Duca Y, La Vignera S, Calogero AE. New insights into the genetics of spermatogenic failure: a review of the literature. Hum Genet 2019;138:125–140.

Chemes HE. Phenotypic varieties of sperm pathology: genetic abnormalities or environmental influences can result in different patterns of abnormal spermatozoa. Anim Reprod Sci 2018;194:41–56.

Chemes HE, Alvarez Sedo C. Tales of the tail and sperm head aches: changing concepts on the prognostic significance of sperm pathologies affecting the head, neck and tail. Asian J Androl 2012;14:14–23.

Chemes HE, Puigdomenech ET, Carizza C, Olmedo SB, Zanchetti F, Hermes R. Acephalic spermatozoa and abnormal development of the head-neck attachment: a human syndrome of genetic origin. Hum Reprod 1999;14:1811–1818.

Chemes HE, Rawe VY. The making of abnormal spermatozoa: cellular and molecular mechanisms underlying pathological spermiogenesis. Cell Tissue Res 2010;341:349–357.

Chen H, Zhu Y, Zhu Z, Zhi E, Lu K, Wang X, Liu F, Li Z, Xia W. Detection of heterozygous mutation in hook microtubule-tethering protein 1 in three patients with decapitated and decaudated spermatozoa syndrome. J Med Genet 2018;55:150–157.

Elkhatib RA, Paci M, Longepied G, Saias-Magnan J, Courbiere B, Guichaoua MR, Levy N, Metzler-Guillemain C, Mitchell MJ. Homozygous deletion of SUN5 in three men with decapitated spermatozoa. Hum Mol Genet 2017;26:3167–3171.

Ihara M, Kinoshita A, Yamada S, Tanaka H, Tanigaki A, Kitano A, Goto M, Okubo K, Nishiyama H, Ogawa O et al. Cortical organization by the septin cytoskeleton is essential for structural and mechanical integrity of mammalian spermatozoa. Dev Cell 2005;8:343–352.

Jarow JP, Sharlip ID, Belker AM, Lipshultz LI, Sigman M, Thomas AJ, Schlegel PN, Howards SS, Nehra A, Damewood MD et al. Best practice policies for male infertility. J Urol 2002;167:2138–2144.

Kim J, Kwon JT, Jeong J, Kim J, Hong SH, Kim J, Park ZY, Chung KH, Eddy EM, Cho C. SPATC1L maintains the integrity of the sperm head-tail junction. EMBO Rep 2018;19:e45991.

Kinoshita M. Assembly of mammalian septins. J Biochem 2003;134:491–496.

Kissel H, Georgescu MM, Larisch S, Manova K, Hunnicutt GR, Steller H. The Sept4 septin locus is required for sperm terminal differentiation in mice. Dev Cell 2005;8:353–364.

Krausz C, Escamilla AR, Chianese C. Genetics of male infertility: from research to clinic. Reproduction 2015;150:R159–R174.

Krausz C, Riera-Escamilla A. Genetics of male infertility. Nat Rev Urol 2018;15:369–384.

Kuo YC, Lin YH, Chen HI, Wang YY, Chiou YW, Lin HH, Pan HA, Wu CM, Su SM, Hsu CC et al. SEPT12 mutations cause male infertility with defective sperm annulus. Hum Mutat 2012;33:710–719.

Kuo YC, Shen YR, Chen HI, Lin YH, Wang YY, Chen YR, Wang CY, Kuo PL. SEPT12 orchestrates the formation of mammalian sperm annulus by organizing core octameric complexes with other SEPT proteins. J Cell Sci 2015;128:923–934.

Lhuillier P, Rode B, Escalier D, Lores P, Dirami T, Bienvenu T, Gacon G, Dulioust E, Toure A. Absence of annulus in human

asthenozoospermia: case report. *Hum Reprod* 2009;**24**: 1296–1303.

Li L, Sha Y, Wang X, Li P, Wang J, Kee K, Wang B. Whole-exome sequencing identified a homozygous BRDT mutation in a patient with acephalic spermatozoa. *Oncotarget* 2017;**8**:19914–19922.

Lin YH, Lin YM, Wang YY, Yu IS, Lin YW, Wang YH, Wu CM, Pan HA, Chao SC, Yen PH *et al*. The expression level of septin12 is critical for spermiogenesis. *Am J Pathol* 2009;**174**:1857–1868.

Liska F, Gosele C, Rivkin E, Tres L, Cardoso MC, Domaing P, Krejci E, Snajdr P, Lee-Kirsch MA, de Rooij DG *et al*. Rat hd mutation reveals an essential role of centrobin in spermatid head shaping and assembly of the head-tail coupling apparatus. *Biol Reprod* 2009; **81**:1196–1205.

Nolan MA, Babcock DF, Wennemuth G, Brown W, Burton KA, McKnight GS. Sperm-specific protein kinase A catalytic subunit Calpha2 orchestrates cAMP signaling for male fertility. *Proc Natl Acad Sci USA* 2004;**101**:13483–13488.

Ono R, Ihara M, Nakajima H, Ozaki K, Kataoka-Fujiwara Y, Taki T, Nagata K, Inagaki M, Yoshida N, Kitamura T *et al*. Disruption of Sept6, a fusion partner gene of MLL, does not affect ontogeny, leukemogenesis induced by MLL-SEPT6, or phenotype induced by the loss of Sept4. *Mol Cell Biol* 2005;**25**:10965–10978.

Oud MS, Volozonoka L, Smits RM, Vissers L, Ramos L, Veltman JA. A systematic review and standardized clinical validity assessment of male infertility genes. *Hum Reprod* 2019;**34**:932–941.

Ounjai P, Kim KD, Lishko PV, Downing KH. Three-dimensional structure of the bovine sperm connecting piece revealed by electron cryotomography. *Biol Reprod* 2012;**87**:73.

Pasek RC, Malarkey E, Berbari NF, Sharma N, Kesterson RA, Tres LL, Kierszenbaum AL, Yoder BK. Coiled-coil domain containing 42 (Ccdc42) is necessary for proper sperm development and male fertility in the mouse. *Dev Biol* 2016;**412**:208–218.

Rawe VY, Terada Y, Nakamura S, Chillik CF, Olmedo SB, Chemes HE. A pathology of the sperm centriole responsible for defective sperm aster formation, syngamy and cleavage. *Hum Reprod* 2002; **17**:2344–2349.

Schatten H. *The Centrosome: Cell and Molecular Mechanisms of Functions and Dysfunctions in Disease*. New York: Humana Press, 2012.

Schatten H, Sun QY. The functional significance of centrosomes in mammalian meiosis, fertilization, development, nuclear transfer, and stem cell differentiation. *Environ Mol Mutagen* 2009;**50**: 620–636.

Schlatt S, Ehmcke J. Regulation of spermatogenesis: an evolutionary biologist's perspective. *Semin Cell Dev Biol* 2014;**29**:2–16.

Sha YW, Sha YK, Ji ZY, Mei LB, Ding L, Zhang Q, Qiu PP, Lin SB, Wang X, Li P *et al*. TSGA10 is a novel candidate gene associated with acephalic spermatozoa. *Clin Genet* 2018;**93**:776–783.

Shen YR, Wang HY, Kuo YC, Shih SC, Hsu CH, Chen YR, Wu SR, Wang CY, Kuo PL. SEPT12 phosphorylation results in loss of the septin ring/sperm annulus, defective sperm motility and poor male fertility. *PLoS Genet* 2017;**13**:e1006631.

Sirajuddin M, Farkasovsky M, Hauer F, Kuhlmann D, Macara IG, Weyand M, Stark H, Wittinghofer A. Structural insight into filament formation by mammalian septins. *Nature* 2007;**449**:311–315.

Sirajuddin M, Farkasovsky M, Zent E, Wittinghofer A. GTP-induced conformational changes in septins and implications for function. *Proc Natl Acad Sci USA* 2009;**106**:16592–16597.

Soley JT. A comparative overview of the sperm centriolar complex in mammals and birds: Variations on a theme. *Anim Reprod Sci* 2016;**169**:14–23.

Sugino Y, Ichioka K, Soda T, Ihara M, Kinoshita M, Ogawa O, Nishiyama H. Septins as diagnostic markers for a subset of human asthenozoospermia. *J Urol* 2008;**180**:2706–2709.

Tokuhiro K, Isotani A, Yokota S, Yano Y, Oshio S, Hirose M, Wada M, Fujita K, Ogawa Y, Okabe M *et al*. OAZ-t/OAZ3 is essential for rigid connection of sperm tails to heads in mouse. *PLoS Genet* 2009;**5**:e1000712.

Tsang CW, Fedchyshyn M, Harrison J, Xie H, Xue J, Robinson PJ, Wang LY, Trimble WS. Superfluous role of mammalian septins 3 and 5 in neuronal development and synaptic transmission. *Mol Cell Biol* 2008;**28**:7012–7029.

Yang K, Meinhardt A, Zhang B, Grzmil P, Adham IM, Hoyer-Fender S. The small heat shock protein ODF1/HSPB10 is essential for tight linkage of sperm head to tail and male fertility in mice. *Mol Cell Biol* 2012;**32**:216–225.

Yeh C-H, Wang Y-Y, Wee S-K, Chen M-F, Chiang H-S, Kuo P-L, Lin Y-H. Testis-specific SEPT12 expression affects SUN protein localization and is involved in mammalian spermiogenesis. *Int J Mol Sci* 2019;**20**:1163.

Yuan S, Stratton CJ, Bao J, Zheng H, Bhetwal BP, Yanagimachi R, Yan W. Spata6 is required for normal assembly of the sperm connecting piece and tight head-tail conjunction. *Proc Natl Acad Sci USA* 2015;**112**:E430–E439.

Zhu F, Liu C, Wang F, Yang X, Zhang J, Wu H, Zhang Z, He X, Zhang Z, Zhou P *et al*. Mutations in PMFBP1 cause acephalic spermatozoa syndrome. *Am J Hum Genet* 2018;**103**:188–199.

Zhu F, Wang F, Yang X, Zhang J, Wu H, Zhang Z, Zhang Z, He X, Zhou P, Wei Z *et al*. Biallelic SUN5 mutations cause autosomal-recessive acephalic spermatozoa syndrome. *Am J Hum Genet* 2016; **99**:1405.